Vol 13 No 9, September 2004
1009-1963/2004/13(09)/1520-06

Chinese Physics

© 2004 Chin. Phys. Soc.
and IOP Publishing Ltd

Monte Carlo simulation of the dynamic evolution of binary lamellar eutectic in directional solidification*

Wang Wei-Min(王伟民)[a)†], Niu Yu-Chao(牛玉超)[a)] Chen Jun-Hua(陈俊华)[a)],
Bian Xiu-Fang(边秀房)[a)], and Liu Jun-Ming(刘俊明)[b)]

[a)] *Key Laboratory of Liquid Structure and Heredity of Materials, Shandong University, Jinan* 250061, *China*

[b)] *Laboratory of Solid State Microstructures, Nanjing University, Nanjing* 210093, *China*

(Received 31 January 2004; revised manuscript received 23 February 2004)

The dynamic evolution of the lamellar eutectic of binary alloys in directional solidification is studied in detail using the Monte Carlo technique. The simulated results can be summarized into two aspects: (1) the lamellar spacing λ is found to be inversely proportional to the chemical potential difference $\Delta\mu$, predicting a linear relationship between the kinetic supercooling $\Delta T_{\rm k}$ and total supercooling at the solid/liquid (S/L) interface; (2) as the solidifying velocity R is low, the dynamic product $\lambda^2 R$ shows a considerable dependence on temperature gradient $G_{\rm T}$ in the liquid in front of the S/L interface, although this dependence becomes much weaker at a high R.

Keywords: eutectic, solidification, Monte Carlo method
PACC: 6150C

1. Introduction

There has been much experimental and theoretical work on the eutectic solidification, which represents one of the classical controlled crystal growth modes in the solidification of the alloys. The foundation for modern theory on eutectic growth was laid by Zener[1] and Brandt[2] in the growth of pearlite, the product of eutectoid reaction in steels. In the 1960s, Jackson and Hunt[3,4] proposed the so-called Jackson–Hunt (JH) theory for the lamellar and rod eutectic growth in directional solidification (DS) of alloys and derived the well-established dynamic relationship $\lambda^2 R$=const, where λ is the lamellar or rod spacing and R is the growth velocity. This theory started from an analysis of solute diffusion in the liquid and the capillary effect of the solidifying interface or solid/liquid (S/L) interface, and predicted the well-accepted relationship among the interface supercooling ΔT, R and λ, i.e. $\Delta T = a_1/\lambda + a_2 R\lambda$, where a_1 and a_2 are constants. The dynamic relationship $\lambda^2 R$=const was derived by utilizing the minimum-supercooling hypothesis. In the 1980s, Datye and Langer[5] started from the JH theory and overcame the limitation of the JH theory by averaging the boundary conditions for the flat S/L interface. In their work, a non-zero temperature gradient $G_{\rm T}$ was introduced. Magnin and Trivedi[6] modified the JH theory by considering the density difference between the two lamellar phases, α and β. Earlier studies concentrated on the solute diffusion in front of the S/L interface, more-or-less making the following assumptions for solving the diffusion equation: (1) the shape of the S/L interface was flat, (2) temperature gradient $G_{\rm T}$ was zero, (3) the kinetic supercooling ΔT_k was negligible.

Considering the stochastic feature of species aggregation on the S/L interface for eutectic solidification, Karma developed a random-walk model to simulate the eutectic growth.[7,8] A convoluted eutectic structure beyond the stable growth condition was predicted in his simulation. However, the Karma model did not include effect of the supercooling on the solidification process, which is the driving force and an important parameter in real growth situation. Later, Xiao *et al*[9] performed Monte Carlo simulations of lamellar eutectic growth, and their model was based on the discretized behaviour of atoms in a complete microscopic sense. The oscillating concentration field in the liquid in front of the S/L interface was simu-

*Project supported by the National Natural Science Foundation of China (Grant Nos 50231040 and 50301008).
†E-mail: weiminw@sdu.edu.cn

lated. Nevertheless, a clear definition of the growth velocity R and the effect of temperature gradient G_{T} were not presented in this model. For lamellar eutectics with two non-faceted lamellar phases, G_{T} does not significantly affect the spacing and lamellar pattern for the S/L interface is roughly isothermal. But for those eutectics with one or two faceted phases, e.g. metal/non-metal alloys such as Al–Si or cast iron alloys, one may argue that the influence of G_{T} cannot be neglected.[10]

In this paper, a Monte Carlo (MC) algorithm is developed to simulate the dynamic evolution of lamellar eutectic structure for a binary system. The major interests are concerned with several matters for improving the understanding of eutectic growth. A positive G_{T} will be imposed onto the liquid in front of the S/L interface, and the effect of G_{T} on the dynamics of eutectic growth will be investigated. We also analyse the dynamic relationship between the lamellar spacing and solidification parameters such as the solidify velocity and temperature gradient.

2. Model and simulation algorithm

2.1. Basic frame

The simulation has been performed in a square lattice of dimensions $l_0 \times l_0$, as shown in Fig.1. The lattice spacing is set equal to unity where periodic boundary conditions are imposed at the lateral end points. The domain is divided into three zones: the liquid regime, and the solid regime which includes α and β phases. In the simulation, the liquid regime is considered as an assembly of empty sites, while liquid species (atoms or molecules) including A and B come from the infinitely distant source. For simplicity, the sources of liquid species are set on source line, far from the solid/liquid (S/L) interface. The solid α phase is composed solely of species A with no solution of species B, and β phase is composed of only species B without A. The thermodynamic framework is quite similar to that proposed by Xiao *et al*[7,8] and has also been described in the authors' previous work.[11,12]

The eutectic solidification procedure includes emission and departure events (in Fig.1): (1) species A or B is emitted from the source line in the liquid regime, undergoes a random walk, then sticks on the S/L interface; (2) species A or B departs from the S/L interface, diffuses along the S/L interface, then escapes from the domain after a random walk. Event (1) may also end by escaping out of the regime, and event (2) may also end by sticking on the S/L interface. Before solidification, 10 layers of the bottom lattices are occupied by species A and B in completely random order. The solidification procedure is operated with one species for each run. The behaviour of the species is determined by the probability of choosing event (1) or event (2).

In the analysis of the simulated results, we define the lamellar spacing (λ) by an average length of $(\alpha+\beta)$ in the lateral direction for a given large number of layers in the solid regime. The growth velocity R is an important parameter, but has not yet been clearly defined previously.[8,9] In our simulation process, we define R as

$$R = \frac{1}{\left[\left(1+\dfrac{N_{\mathrm{de}}}{N_{\mathrm{st}}}\right) n_{\mathrm{mc}}\right]^{3/2}} + a_0, \qquad (1)$$

where the numerator of the first term on the right-hand side is unit length of solidification; N is the needed number of species and n_{mc} is the total MC steps for the solidified layers in unit length, the subscripts st and de denote the species that have stuck on the interface (occupying the S/L sites) and the ones, departed from the interface, respectively, and a_0 is a constant. Since our simulation is performed in a two-dimensional lattice and one species has 4 possible directions of movement, while the realistic solidification proceeds in three-dimensional space and six directions of movement are allowed, the exponential for the first term in Eq.(1) is set as 3/2. $N_{\mathrm{de}}/N_{\mathrm{st}}$ is a parameter scaling the interface diffusion. When N_{de} is very small, all species in the liquid can stick onto the solidifying interface irreversibly, implying that nearly no interface diffusion occurs and R is large; when N_{st} is very small compared with N_{de}, the interface diffusion will dominate the solidification and R is low. In our simulation, we find the system solidifies with a very slow velocity R_{c} at a small $\Delta\mu$ (where $\Delta\mu$ is the chemical potential difference between the solid and liquid), and the solidification will stop if $\Delta\mu$ somewhat decreases. Accordingly we set $a_0 = -R_{\mathrm{c}}$ which is strongly dependent on the distance from S/L interface to the source line. Similar to the other MC simulations,[13,14] it is difficult to scale R by a length/time unit, as happens in the experimental case. Accordingly a relative unit (R.U.) is used to scale R.

2.2. Chemical potential and temperature gradient

Firstly, a random number $R_{\rm m}$ is produced and the probability $P_{\rm e}$ is calculated for the system to choose either a departure event or an emission event, the expression of $P_{\rm e}$ is based on the symmetrical solution.[15] Accordingly, we obtain

$$0 < R_{\rm m} < P_{\rm e} = \frac{1}{1+\exp(\Delta\mu/k_{\rm B}T)}, \qquad (2a)$$

for departure event

$$P_{\rm e} = \frac{1}{1+\exp(\Delta\mu/k_{\rm B}T)} < R_{\rm m} < 1, \qquad (2b)$$

for emission event

where $k_{\rm B}$ is the Boltzmann constant and T is temperature.

Unlike previous models,[7,8] a non-zero temperature gradient is imposed on the S/L interface by including it in the expression for the local attachment probability on the S/L interface for a species. Another random number $R_{\rm m}$ is produced and also determines the local attachment probability based on the symmetrical solution, and we acquire

$$0 < R_{\rm m} \le P_{\rm s} = \frac{\exp(\Delta\mu/k_{\rm B}T)\exp[(\Delta E_{\rm bond} - G_{\rm T}\Delta l)/k_{\rm B}T]}{1+\exp(\Delta\mu/k_{\rm B}T)\exp[(\Delta E_{\rm bond} - G_{\rm T}\Delta l)/k_{\rm B}T]}, \quad \text{for sticking process} \qquad (3a)$$

$$P_{\rm s} = \frac{\exp(\Delta\mu/k_{\rm B}T)\exp[(\Delta E_{\rm bond} - G_{\rm T}\Delta l)/k_{\rm B}T]}{1+\exp(\Delta\mu/k_{\rm B}T)\exp[(\Delta E_{\rm bond} - G_{\rm T}\Delta l)/k_{\rm B}T]} < R_m < 1, \quad \text{for diffusion process} \qquad (3b)$$

where $\Delta E_{\rm bond} = \phi_{\alpha\alpha}n_{\alpha\alpha} + \phi_{\beta\beta}n_{\beta\beta} + \phi_{\alpha\beta}n_{\alpha\beta}$, here $\phi_{\alpha\alpha}$, $\phi_{\beta\beta}$, and $\phi_{\alpha\beta}$ are the bond energies for A–A pairs, B–B pairs and A–B pairs, respectively, $n_{\alpha\alpha}$, $n_{\beta\beta}$, and $n_{\alpha\beta}$ are the numbers of the updated nearest-neighbor bonds of A–A pairs, B–B pairs, and A–B pairs after attachment of one species onto the S/L interface, respectively; Δl is the distance of the attaching location away from the S/L interface with an average height $l_{\rm av}$ in the growth direction (see Fig.1). The interface diffusion probability of one species is

$$P_{i\to j} = \exp(-\Delta E_{i\to j}/k_{\rm B}T)/\sum_{j=1}^{n}\exp(-\Delta E_{i\to j}/k_{\rm B}T), \qquad (4)$$

where $\Delta E_{i\to j}$ is the total energy difference of the species before and after transferring from site i to site j, n is the number of the unoccupied nearest-neighbors of site i, including site i itself.

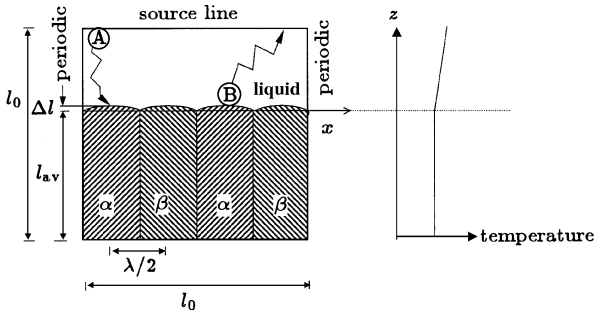


Fig.1. The domain of the MC simulation model (Solidification direction is from bottom to top of figure).

2.3. SOS restriction

In the present simulation, the solid-on-solid (SOS) assumption is employed too.[8–11] The simulation is ended after a given number of species are deposited on the solidifying S/L interface. The parameters used in the modelling are listed in Table 1.

Table 1. Parameters for the present MC simulation.

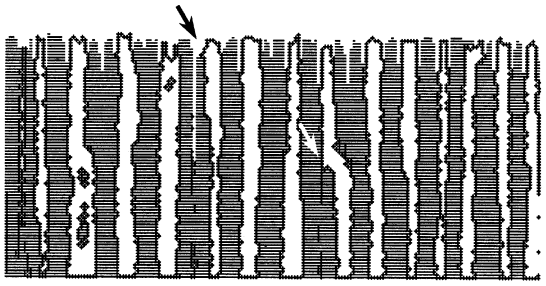
l_0	$l_{\rm av}$	$\phi_{\rm AA}/k_{\rm B}T$	$\phi_{\rm BB}/k_{\rm B}T$	$\phi_{\rm AB}/k_{\rm B}T$	$G^*_{\rm T}/k_{\rm B}T$	c_0	$\Delta\mu/k_{\rm B}T$
180	50∼90	1.5	1.5	-8.5	0∼4.0	0.7	8.0∼1.0

*The full form of unit of $G_{\rm T}$ is $k_{\rm B}T/b$, where b is lattice spacing, which is set equal to unity.

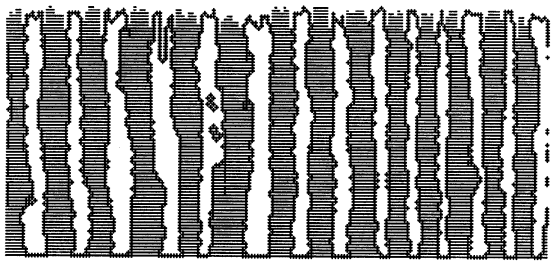
3. Results and discussion

3.1. Variation of lamellar pattern

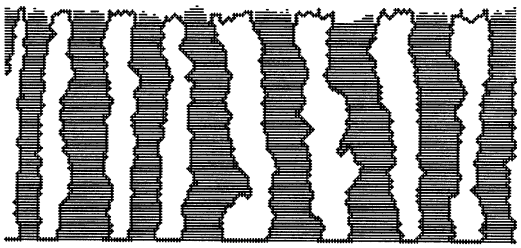
Figure 2 shows the simulated lamellar patterns at various values of $\Delta\mu$. The lamellar spacing increases with decreasing $\Delta\mu$. Especially, at a high $\Delta\mu$, the solidifying interface is seriously irregular and some liquid zones extend into the A-B phase (see the black arrow in Fig.2(a)). At the same time, the convoluted eutectic texture (see the white arrow in Fig.2(b)) is similar to the simulated results of Karma[7] and the observed pattern in CBr_4-C_2Cl_6 by Jackson and Hunt.[3] This structure implies that the lamellar eutectic growth is destabilized due to the instability of the S/L interface, which is very often observed in real systems.



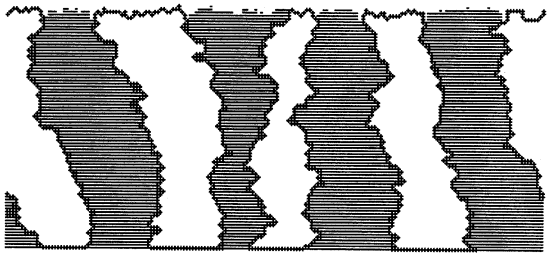
(a) $\Delta\mu$=8$k_{\rm B}T$



(b) $\Delta\mu$=6$k_{\rm B}T$



(c) $\Delta\mu$=4$k_{\rm B}T$



(d) $\Delta\mu$=2$k_{\rm B}T$

Fig.2. Patterns with different chemical potential ($G_{\rm T}$=1.0 $k_{\rm B}T$, α-dark zone, β-bright zone, solidification direction is from bottom to top of the figure).

According to the JH theory,[3] one has the following relationships:

$$\Delta T = \frac{a_1}{\lambda} + a_2 R\lambda. \tag{5}$$

Applying the minimal supercooling hypothesis, Eq.(5) gives

$$\lambda \propto R^{-1/2}. \tag{6}$$

Meanwhile, we can obtain

$$\Delta T = K\frac{1}{\lambda}, \tag{7a}$$

$$\Delta T = KR^{1/2}, \tag{7b}$$

where K is a constant, and the total supercooling ΔT at the solidifying interface is the difference between the eutectic temperature $T_{\rm e}$ and the actual temperature of S/L interface.

Generally, ΔT consists of three parts:[3,6] (1) the constitutional (or solute) supercooling $\Delta T_{\rm c}$, which reflects the fact that the composition in the liquid at S/L interface locally slightly departs from the eutectic composition, leading to a deviation of the equilibrium temperature from the eutectic temperature; (2) the capillary supercooling $\Delta T_{\rm r}$, which obeys the Gibbs–Thomson law; (3) the kinetic supercooling $\Delta T_{\rm k}$, which represents the difference between the chemical potentials of the liquid and solid phases at the interfaces, i.e. the driving force for the attachment kinetics. When the growth velocity is very low, $\Delta T_{\rm k}$ can be neglected. In our simulation, $\Delta T_{\rm k}$ counts and is denoted by the chemical potential difference, $\Delta\mu$. We find the averaged lamellar spacing $\lambda_{\rm av}$ is inversely proportional to $\Delta\mu$, shown in Fig.3, which is consistent with Eq.(7a). This implies that the relationship between $\Delta\mu$ (namely $\Delta T_{\rm k}$) and ΔT is linear. Accordingly, neglecting of $\Delta T_{\rm k}$ does not essentially change the conclusion since $\Delta T_{\rm k}$ (and $\Delta\mu$) only affects the value of constants a_1 and a_2 in Eq.(3). From Fig.3, it is found that the distribution range of λ is wide when $\Delta\mu$ is low, which compares well with the theoretical prediction of Shingu [16] and the experimental results of Ourdjini *et al.*[17] In addition, the role of $\Delta\mu$ in the JH model may possibly extend the model to the eutectic growing situation in the absence of constitutional supercooling, like PVD[18], PLD[19] and other methods.

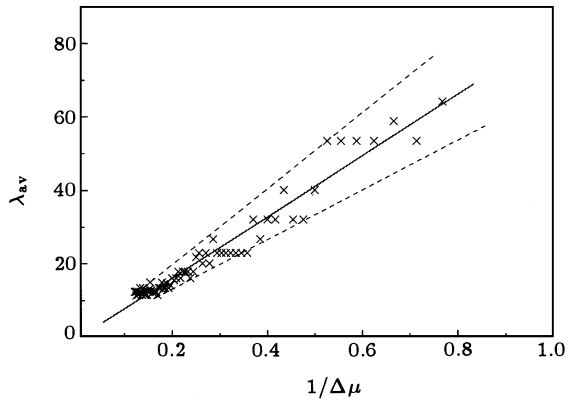


Fig.3. Variation of $\lambda_{\rm av}$ with $1/\Delta\mu$ ($G_{\rm T}$=1.0 $k_{\rm B}T$).

Figure 4 shows the approximately linear relationship between $R^{1/2}$ and $\Delta\mu$. According to the linear

relationship between $\Delta\mu$ and ΔT, we can obtain that the simulated $R^{1/2}$ is linear with ΔT, corresponding well to Eq.(7b). This indicates that the expression for the growth velocity (Eq.(1)) is reasonable. From Fig.4, when $\Delta\mu$ is fairly low, R appears obviously lower and deviates from the linear curve. In Kassner and Misbah's[20] and our previous works,[21] the product of $\lambda^2 R$ is found to be equal to a constant in a wide range of R, while it deviates from the constant with decreasing R when R is low enough, which is in accordance with the deviation of the simulated R at a low $\Delta\mu$ in Fig.4. In the abnormal eutectic growth of Al–Si alloy, Elliott and Glenister[22] proposed the relationship between velocity and supercooling as

$$\Delta T = 2.24R^{0.25}$$

at low velocities for the coarse silicon, (8a)

$$\Delta T = 0.80R^{0.50}$$

at high velocities for the finer flake silicon. (8b)

The experimental deviation from $\Delta T \propto R^{f1/2}$ also occurs at a low velocity (shown in Fig.4), when Si phase is coarse, implying that the growth is much more anisotropic than at high velocities. It is found also that the shape of experimental $R^{1/2} - \Delta T$ curve is similar to that of our simulated $R^{1/2} - \Delta\mu$, implying that the present simulation is reasonable and of forecasting capability.

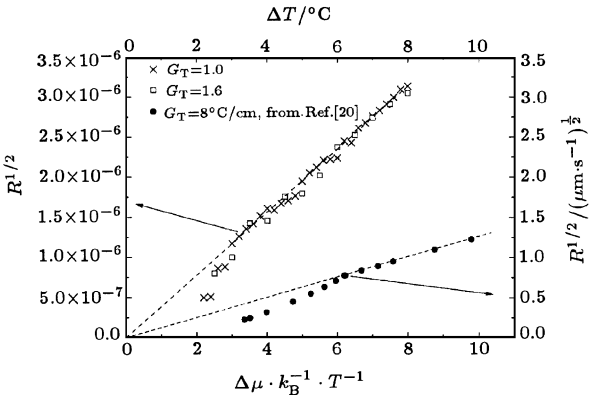


Fig.4. The linear relation of the velocity $R^{1/2}$ vs $\Delta\mu$ (×: G_T=1.0 k_BT; □: 1.6 k_BT; •: from $\Delta T = 2.24R^{0.25}$ at low velocities and ΔT=$0.80R^{0.50}$ at high velocities in Ref.[22]).

3.2. Influence of temperature gradient G_T

It has been demonstrated in many experiments that the influence of G_T is considerable, in particular for those systems containing one or more faceted phases.[10] Kassner and Misbah[20,23] derived a nonlinear similarity equation from the full boundary integral equation, predicting that the dynamic product $\lambda^2 R$ decreases with increasing G_T, for a fixed R. Figure 5 shows the calculated $\lambda^2 R$ as a function of G_T at various R. Indeed $\lambda^2 R$ changes linearly with G_T at a negative slope. The numerical calculation of our previous work by limited differential method[11] also confirmed this argument. It is proposed that the following relationship exists between $\lambda^2 R$ and G_T:

$$\lambda^2 R = a_3 \exp(-a_4 G_T/R), \tag{9}$$

where a_3 and a_4 are two positive constants, Eq.(9) may be decomposed into Taylor's series as

$$\begin{aligned}\lambda^2 R =& a_3 \exp(-a_4 G_T/R)\\ =& a_3 \left[1 - a_4 G_T/R + \frac{(-a_4 G_T/R)^2}{2!} + \cdots \right.\\ &\left. + \frac{(-a_4 G_T/R)^n}{n!} + \cdots \right],\end{aligned} \tag{10}$$

for $G_T \ll R/a_4$, the terms $(-a_4 G_T/R)^n/n!$ with higher order ($n \geq 2$) may be omitted, and it gives

$$\lambda^2 R \approx a_3[1 - a_4 G_T/R]. \tag{11}$$

From Eq.(11), $\lambda^2 R$ and G_T show a linear relationship when R is low, and the slope of the curve $\lambda^2 R - G_T$ is negative. This is also shown in the simulated results in Fig.5(c). For Al–Si alloys, it has been found experimentally that the empirical effect of G_T can be written as[24]

$$\lambda \approx AR^{-1/2}G_T^{-1/3}, \quad \Delta T \approx BR^{1/2}G_T^{-1/2}, \tag{12}$$

where A and B are constants. Because of the complexity of the irregular growth of Al–Si alloys, Eq.(12) is not completely similar to Eq.(11), but it also shows that $\lambda^2 R$ decreases with increase of G_T as seen in Eq.(11).

In addition, when R increases and $a_4 G_T/R \ll 1$, Eq.(11) is converted to

$$\lambda^2 R \approx a_3, \tag{13}$$

which is identical to the well known JH arguments (see Eq.(6)). This is well supported by the simulation results, shown in Figs.5(a) and 5(b). Figure 6 shows the variation of slope of $\lambda^2 R - G_T$ curve calculated from Eq.(9) and the present simulated results. In the case of the small R values, the slope of $\lambda^2 R - G_T$ increases with R, while its absolute value decreases. When R increases, the slope will not increase continually but tend to zero when R is large enough. The present simulated results fit well the curve from Eq.(9), which reflects two cases indicated by Eqs.(11) and (13).

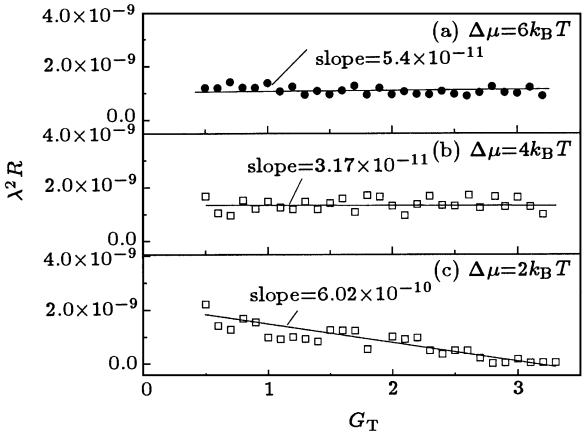


Fig.5. Variation of the product $\lambda^2 R$ with G_T at different $\Delta\mu$.

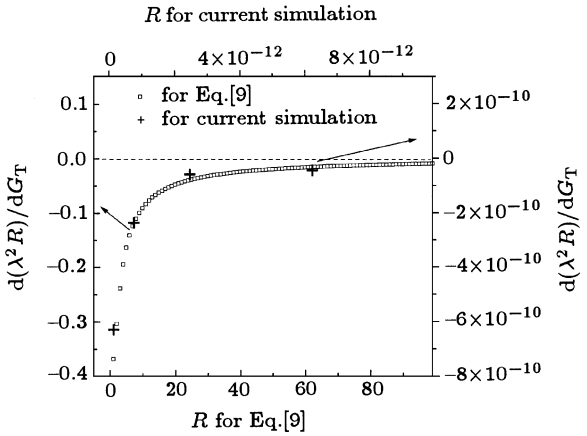


Fig.6. Variation of $d(\lambda^2/R)/dG_T$ with R (□ for Eq.(9), + for current simulation).

4. Conclusions

In conclusion, we have used the MC method to simulate the phase-separated patterns in the directional solidification of eutectic alloys. We find lamellar spacing λ is in linear relationship with the reciprocal of chemical potential difference $\Delta\mu$, suggesting that the kinetic supercooling ΔT_k is also linear to the total supercooling. The simulated $R^{1/2}$ is also linear to $\Delta\mu$ except that R is very low. At a very high R, the convoluted structure occurs, implying that the boundary layer deviates from the steady state and the interface instability occurs. In our simulation, the product $\lambda^2 R$ decreases with increasing G_T at a low R, while the product tends to be independent of G_T when R is high enough.

References

[1] Zener C 1946 *AIME Trans.* **167** 550.
[2] Brandt W H 1945 *J. Appl. Phys.* **16** 139
[3] Jackson K A and Hunt J D 1966 *Trans. Met. Soc. AIME* **236** 1129
[4] Hunt J D and Jackson K A 1966 *Trans. Met. Soc. AIME* **236** 843
[5] Datye V and Langer J S 1966 *Phys. Rev.* B **24** 4155
[6] Magnin P and Trivedi R 1991 *Acta Mater.* **39** 453
[7] Karma A 1987 *Phys. Rev. Lett.* **59** 71
[8] Xiao R F, Alexander J I D and Rosenberger F 1994 *Mater. Sci. Eng.* A **178** 23
[9] Xiao R F, Alexander J I D and Rosenberger F 1992 *Phys. Rev.* A **45** R571
[10] Toloui B and Hellawell A 1976 *Acta Metall.* **24** 565-573
[11] Liu J M, Wu Z C and Liu Z G 1998 *Script. Mater.* **38** 715
[12] Wang W M, Liu J M, Chen X Y and Liu Z G 2002 *J. Cryst. Growth* **240** 313
[13] Heermann D W 1989 *Computer Simulation Methods in Theoretical Physics* (Berlin: Springer)
[14] Das A and Mittemeijer E J 2000 *Metall. Mater. Trans.* **31A** 2049
[15] Hirosawa S and Sato T 2001 *Model. Simul. Mater. Sci. Eng.* **9** 129
[16] Shingu P 1979 *J. Appl. Phys.* **50** 5743
[17] Ourdjini A, Liu J and Elliott R 1994 *Mater. Sci. Tech.* **10** 312
[18] Zhao L Z, Shen M Y and Goto T 2001 *Acta Phys. Sin.* **50** 1540 (in Chinese)
[19] Zou L, Wang L, Huang J Y, Zhao B H and Ye Z Z 2003 *Acta Phys. Sin.* **52** 935 (in Chinese)
[20] Kassner K and Misbah C 1991 *Phys. Rev.* A **44** 6533
[21] Liu J M, Liu Z G and Wu Z C 1993 *Mater. Sci. Eng.* A **167** 87
[22] Elliot R and Glenister S M D 1980 *Acta Metall.* **28** 1489
[23] Kassner K and Misbah C 1991 *Phys. Rev. Lett.* **66** 445
[24] Hogan L M and Song H 1987 *Metall. Trans.* **18A** 707